



HAL
open science

Modelling the mechanical behaviour of a carbon/carbon composite material for aeronautical structures under the influence of its environment

Mathias Rahard, Myriam Kaminski, Jean-François Maire, Frédéric Laurin,
Florent Bouillon, Vasile-Ionut Prisacari

► To cite this version:

Mathias Rahard, Myriam Kaminski, Jean-François Maire, Frédéric Laurin, Florent Bouillon, et al.. Modelling the mechanical behaviour of a carbon/carbon composite material for aeronautical structures under the influence of its environment. ECCM 2024, Jul 2024, Nantes, France. hal-04669354

HAL Id: hal-04669354

<https://hal.science/hal-04669354v1>

Submitted on 8 Aug 2024

HAL is a multi-disciplinary open access archive for the deposit and dissemination of scientific research documents, whether they are published or not. The documents may come from teaching and research institutions in France or abroad, or from public or private research centers.

L'archive ouverte pluridisciplinaire **HAL**, est destinée au dépôt et à la diffusion de documents scientifiques de niveau recherche, publiés ou non, émanant des établissements d'enseignement et de recherche français ou étrangers, des laboratoires publics ou privés.

MODELLING THE MECHANICAL BEHAVIOUR OF A CARBON/CARBON COMPOSITE MATERIAL FOR AERONAUTICAL STRUCTURES UNDER THE INFLUENCE OF ITS ENVIRONMENT

M. Rahard¹, M. Kaminski¹, J.-F. Maire¹, F. Laurin¹,
F. Bouillon², V.-I. Prisacari³

¹DMAS, ONERA, Université Paris-Saclay, 92320, Châtillon, France
Email : mathis.rahard@onera.fr

²Safran Ceramics, a technology platform of Safran Tech,
105 avenue Marcel Dassault 33700 Mérignac , France
Email : florent.bouillon@safrangroup.com

³Safran Landing Systems, 7 rue Général Valérie André, 78140, Vélizy-Villacoublay, France
Email : vasile-ionut.prisacari@safrangroup.com

Keywords: Carbon/Carbon, Oxidation, Damage, Modeling

Abstract

The study focuses on developing a model for the specific lifetime of Carbon/Carbon (C/C) ceramic matrix composites in aeronautics braking systems, considering the effect of carbon oxidation on the thermo-mechanical properties. During the landing and taxi-out phases, brake temperatures range from 400°C to 800°C, leading to significant oxidation reactions with atmospheric oxygen. The literature review and the tests carried out in this study show that the duration but also the temperature of oxidation affect the mechanical properties. An in-depth understanding and advanced modeling approach are required to explain the results obtained. The modeling involves two main steps. First, the oxidation state of the material is estimated considering the environmental conditions. Then, the effects of oxidation on the mechanical properties are considered. A thermodynamically consistent behavior law based on the continuum damage framework has been developed, considering both the effects of mechanical loading and oxidation. The predictions of the model have been compared with the available test results and is able to reproduce the observed trends.

1. Introduction

Carbon-Carbon (C/C) composites are Ceramic Matrix Composites (CMCs), but with some specificities compared to classical C/SiC or SiC/SiC material [1]. C/C composites have found many applications in the aerospace industry. For instance, in nose cones for reentry vehicles and ballistic missiles, as well as in the leading edge of the Space Shuttle and in aircraft braking systems which represent the largest consumption of this material. The latter is the practical application of the material in this study which constitutes the heat sink of the brake, as shown in Figure 1 [2], which captures the heat generated by braking, thus protecting other parts sensitive to high temperatures. However, C/C composite is susceptible to oxidation phenomena. Above 400°C, oxygen reacts strongly with carbon, which consumes the composite and degrades its mechanical properties. The C/C composite studied is a needle-punched 2.5D preform stacked in [0/±60] orientations, then densified by a CVI (Chemical Vapor Infiltration) process. The microstructure of the material under study is similar to that shown in Figure 2.

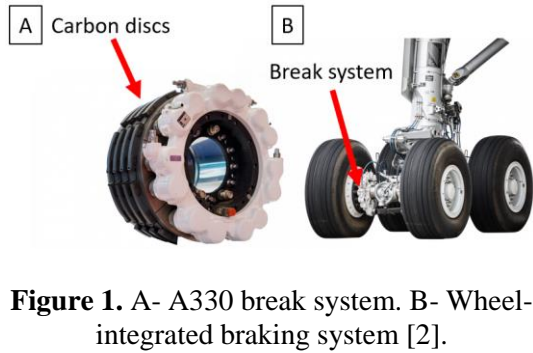


Figure 1. A- A330 break system. B- Wheel-integrated braking system [2].

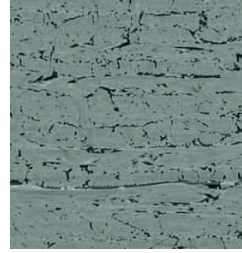


Figure 2. Material microstructure [3].

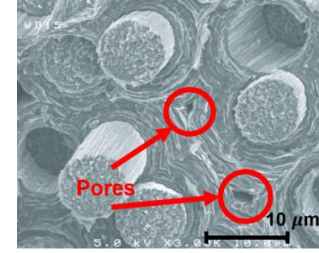


Figure 3. Pores due to CVI process [4].

The CVI densification process generates pores, as shown in Figure 3 [4], which facilitate oxidation and this promotes the degradation of the mechanical properties. Therefore, the aim of this study is to propose a constitutive law able to describe the evolution of the mechanical properties (rigidity and damage) as a function of the oxidation. Firstly, the definition and the modelling of the oxidation state in /C composites is provided. Then, the influence of the oxidation on elastic properties and on the damage process are described. Finally, the model predictions are compared with experimental data.

2. Modeling the influence of oxidation on the mechanical behavior

2.1. Formalism for describing the oxidation state

The rate of oxidation is usually estimated by measuring the loss of mass, noted as Δm , compared to the mass of the material after manufacture. In standard application of brakes, the oxidation rate, also known as burn-off, does not normally exceed 5%. For C/C materials, three oxidation domains can be distinguished. Below 400°C, the oxidation reaction is not activated or takes a very long time. Between 400°C and 800°C, it can be reasonably assumed that oxidation is mainly uniform throughout the volume, due to the considerable pore rates. Above 800°C, surface oxidation phenomena predominate over volume mechanisms. In this study, the temperature range for describing oxidation corresponds to the second domain. The overall oxidation kinetics of C/C materials, denoted by the variable Δm , is assumed to follow an Arrhenius law [5], as reported in Eq 1., where E_a is the activation energy, the R perfect gas constant, T the temperature, and A a material parameter to be defined :

$$\dot{\Delta m} = A \exp\left(-\frac{E_a}{RT(t)}\right) \quad (1)$$

Nevertheless, for the same mass loss obtained at different oxidation temperatures, the effect of oxidation on the mechanical properties are different, as shown in Figures 4 and 5. This means that the global variable Δm is not sufficient to describe the oxidation rate.

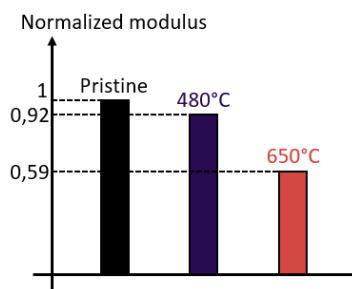


Figure 4. Effect of oxidation ($\Delta m = 5\%$) on the Young's modulus of the material under study.

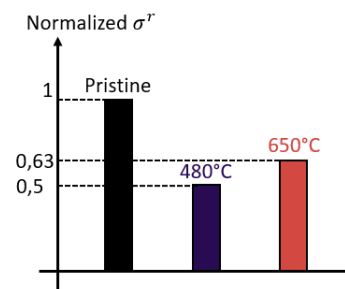


Figure 5. Effect of oxidation ($\Delta m = 5\%$) on the material's tensile strength σ^r .

To take account of this specificity, the idea is to create as many oxidation state variables as there are oxidation mechanisms to be described. In a first time, only two variables, homogeneous as mass loss, are considered : one to describe mechanisms occurring at low oxidation temperature (400°C), denoted Δm_1 , and a second, Δm_2 , for those occurring at higher temperature (800°C). Eq. 2 defines the evolution of these variables, and their relation to the measured global mass loss :

$$\Delta \dot{m} = \Delta \dot{m}_1 + \Delta \dot{m}_2 \quad \text{and} \quad \begin{cases} \Delta \dot{m}_1 = \zeta(T) \Delta \dot{m} \\ \Delta \dot{m}_2 = (1 - \zeta(T)) \Delta \dot{m} \end{cases} \quad (2)$$

The term ζ corresponds to a logistic function, that allows the transition from one oxidation mechanism to another as a function of the oxidation temperature, as given in Eq. 3.

$$\zeta(T) = \frac{1}{2} (1 - \tanh(\gamma(T - T_c))) \quad (3)$$

Two coefficients control the transition between oxidation mechanisms: γ to calibrate the transition rate and T_c to define the transition temperature, as shown in Figure 6.

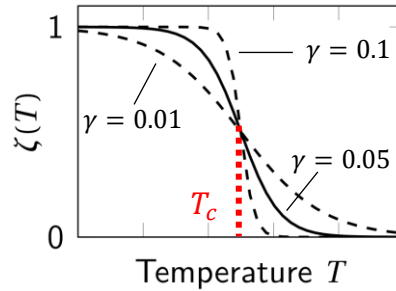


Figure 6. Representation of the logistic function ζ

Thanks to the introduction of the two variables Δm_1 and Δm_2 , it is now possible to attribute different effects of oxidation on mechanical properties at low and high temperatures. Indeed, it is clear that the oxidation mechanisms associated with Δm_1 will predomine at temperatures lower than T_c , and vice versa the oxidation mechanisms associated with Δm_2 will predomine for temperatures higher than T_c .

2.2. Evolution law of the elastic compliance tensor due to oxidation without damage

In this part, we consider only the linear elastic part of the behavior (Eq. 4). The tensor \mathbb{S}^0 is the elastic compliance tensor at the initial state. The tensor \mathbb{S}^{Ox} corresponds to the one after oxydation. So, without oxydation $\Delta m = 0$, the two tensors are equal, meaning $\mathbb{S}^{\text{Ox}} = \mathbb{S}^0$.

$$\boldsymbol{\varepsilon} = \mathbb{S}^{\text{Ox}}(T, \Delta m_k) : \boldsymbol{\sigma} \quad (4)$$

The objective is to establish a law describing the evolution of the oxidized tensor \mathbb{S}^{Ox} as a function of temperature and the two mass losses associated to the different mechanisms. Considering the evolution of the compliance tensor as a function of time is a convient framework, as reported in Eq 5.

$$\frac{d\mathbb{S}^{\text{Ox}}(T, \Delta m_k)}{dt} = \frac{\partial \mathbb{S}^{\text{Ox}}}{\partial T} \dot{T} + \sum \frac{\partial \mathbb{S}^{\text{Ox}}}{\partial \Delta m_k} \Delta \dot{m}_k \quad (5)$$

As described in Eq. 5, the evolution of the oxidized tensor due to the temperature is distinguished from the evolution due to the oxidation mechanisms. Firstly, the definition of the temperature-induced

variation of the compliance tensor is considered. Temperature has a particular effect on the C/C elastic stiffness. Research studies in the literature [4,6] indicate that the apparent stiffness increases with temperature up to about 1500°C, after which it decreases sharply, as shown in Figures 7 and 8.

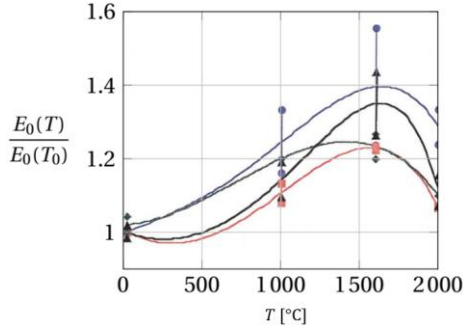


Figure 7. Effect of temperature on the stiffness of a C/C material [4]

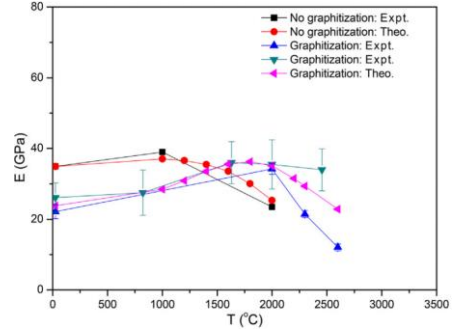


Figure 8. Effect of temperature and graphitization on the stiffness of a C/C material [6]

For now, the Young's modulus E_i and the shear modulus G_{ij} are assumed to be affected in the same way. The Poisson's ratios ν_{ij} are assumed to be constant due to measurement issues during experimental tests. It means that all coefficients of \mathbb{S}^{Ox} are affected in the same manner. The chosen analytical expression for the Young's modulus is given by Eq. 6.

$$E^{\text{Ox}}(T, \Delta m_k) = E^{\text{Ox}}(T_0, \Delta m_k) \left(\frac{1}{1 + \exp\left(\frac{T - T_s}{\alpha}\right)} + (T - T_0)\beta \right) \quad (6)$$

The coefficient T_s corresponds to the temperature at the maximum stiffness, α controls the shape of the peak, β controls the stiffness increase before the peak and T_0 is the ambient temperature.

Secondly, a definition of the oxidation-induced variation of the compliance tensor is considered. An expression for the evolution of the tensor \mathbb{S}^{Ox} due to oxidation is given by Eq. 7.

$$\sum \frac{\partial \mathbb{S}^{\text{Ox}}}{\partial \Delta m_k} \Delta \dot{m}_k = \mathbb{S}^0(T) g(\Delta \dot{m}_k) \quad (7)$$

The effect of the oxidation on the evolution of the tensor \mathbb{S}^{Ox} is governed by the scalar function g expressed in Eq. 8. Two coefficients have been introduced : ξ_1 to calibrate the effect of the oxidation mechanism $\Delta \dot{m}_1$ on $\dot{\mathbb{S}}^{\text{Ox}}$ and ξ_2 to calibrate the effect of $\Delta \dot{m}_2$.

$$g(\Delta \dot{m}_k) = \xi_1 \Delta \dot{m}_1 + \xi_2 \Delta \dot{m}_2 \quad (8)$$

To illustrate the oxidation process, let us consider an oxidation that takes place in an isothermal environment, *i.e.* $\dot{T} = 0$, and the temperature rise is instantaneous, as shown in Figure 9. The temperature T_{Ox} is the oxidation temperature. The time t_0 corresponds to the initial state and t_1 to the start of oxidation. The time $t_{\Delta m}$ corresponds to the time required to reach an oxidation rate of Δm and t is the current time after oxidation. Eq. 5 can be integrated with respect to the time through the oxidation path, between t_0 and $t > t_{\Delta m}$. At ambient temperature T_0 , the material is not oxidized, or according to the Arrhenius law, over an extremely long time. So, the variation of \mathbb{S}^{Ox} between t_0 and t_1 as well as between $t_{\Delta m}$ and t can be neglected.

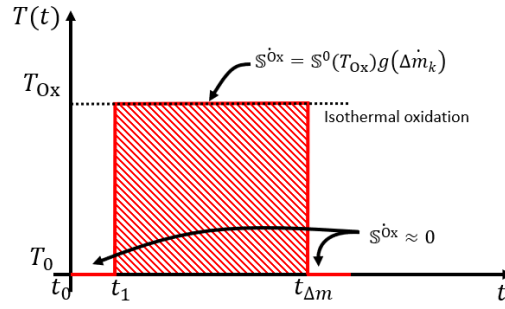


Figure 9. Thermal loading of the example

The calculations lead to Eq. 9, which describes the evolution of the normalized elastic modulus as a function of the oxidation rate, depending on the oxidation temperature T_{Ox} .

$$\begin{cases} \Delta m_1 = \zeta(T_{Ox})\Delta m \\ \Delta m_2 = (1 - \zeta(T_{Ox}))\Delta m \\ g(\Delta m_k) = \xi_1 \Delta m_1 + \xi_2 \Delta m_2 \\ \frac{E^{Ox}(T_{Ox}, \Delta m_k)}{E^0(T_{Ox})} = \frac{1}{1 + g(\Delta m_k)} \Leftrightarrow \frac{E^{Ox}(T_0, \Delta m_k)}{E^0(T_0)} = \frac{1}{1 + \frac{E^0(T_0)}{E^0(T_{Ox})}g(\Delta m_k)} \end{cases} \quad (9)$$

The expression for the shear modulus evolution is similarly assumed. Figure 10 shows the effect of the oxidation temperature T_{Ox} on the Young's modulus for several values of global mass loss. The purple crosses represent experimental measurements made at $\Delta m = 5\%$ for oxidation temperatures equal to 480°C and 650°C. The shape of the curves depends on the material coefficients γ , T_c , ξ_1 and ξ_2 . For now, the lack of experimental data makes the identification of these coefficients difficult. Nevertheless, this model effectively describes the effects of oxidation on the elastic properties at low and high oxidation temperatures for a given mass loss. The decrease in the apparent modulus, shown in Figure 11, is similar to test results found in the literature for another C/C material [7].

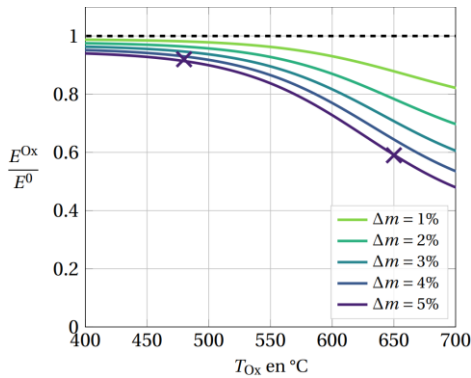


Figure 10. Evolution of the elastic modulus relative to the initial modulus as a function of T_{Ox} for several Δm .

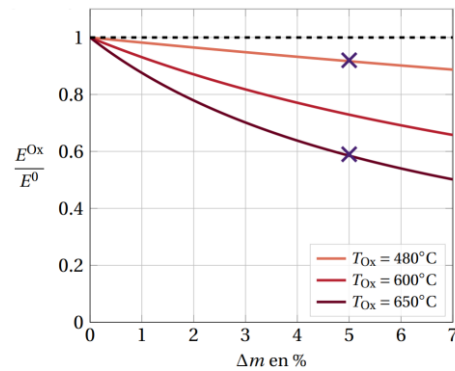


Figure 11. Evolution of the elastic modulus relative to the initial modulus as a function of Δm for several T_{Ox} .

2.3. Effect of oxidation on damage

The model considered to take into account the effect of damage on the material behaviour is ODM for Onera Damage Model. This model was developed for static loading [9], and more recently for fatigue [10]. In this paper, only the static one part is considered for simulations. Some details about the

behaviour law, provided in Eq. 10, are given below. More details are provided in the literature [8,9,10].

$$\begin{aligned} \boldsymbol{\sigma} &= \mathbb{C}^{\text{eff}} : (\boldsymbol{\varepsilon} - \boldsymbol{\varepsilon}_0) + \mathbb{C}^{\text{Ox}} : \boldsymbol{\varepsilon}_0 \\ \mathbb{C}^{\text{eff}} &= (\mathbb{S}^{\text{eff}})^{-1} = \left(\mathbb{S}^{\text{Ox}} + \sum d_i \mathbb{H}_i \right)^{-1} \\ d_i &= (d_i^\infty - d_i) \left\langle \frac{\varepsilon_{\text{eq}_i}^{\text{max}} - \varepsilon_{\text{eq}_i}^{\text{os}}}{S_i^S} \right\rangle_+^{\beta_i^S} \left\langle \dot{\varepsilon}_{\text{eq}_i}^{\text{max}} \right\rangle_+ \text{ and } \varepsilon_{\text{eq}_i} = \sqrt{y_i} \end{aligned} \quad (10)$$

Where $\boldsymbol{\sigma}$ is the stress, $\boldsymbol{\varepsilon}$ the total strain, $\boldsymbol{\varepsilon}_0$ the closure strain and \mathbb{C}^{Ox} the non-oxidized elastic stiffness tensor. The effective tensor \mathbb{C}^{eff} is degraded during the mechanical loading above a certain damage threshold. The scalar variables d_i are the damage variables representing the matrix meso-damages oriented at 0° , $\pm 45^\circ$ and 90° and an additional variable is considered through the out-of-plane direction of the material. The evolution of these variables is defined by non-linear differential equations, reported in Eq. 10. The different material parameters to be identified with the mechanical tests are: a threshold (occurrence of the first crack) y_{0_i} , the kinetics of the damage evolution y_{c_i} , and the damage saturation d_i^∞ . \mathbb{H}_i are the effect tensors identified by homogenisation [8], using the elastic properties of the material. They are defined in such a way that the damage variables affect the elastic properties only when the cracks are opened, i.e. the unilateral aspect of the damage is guaranteed.

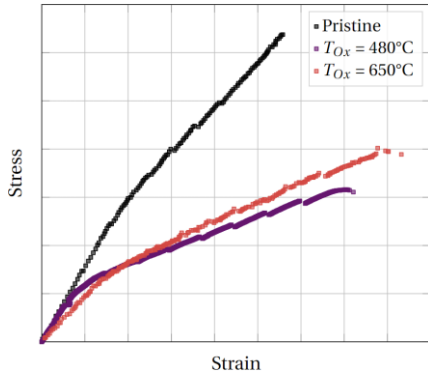


Figure 12. Envelope of the behaviour curves of the pristine and oxidized material ($\Delta m = 5\%$) for two different oxidation temperatures.

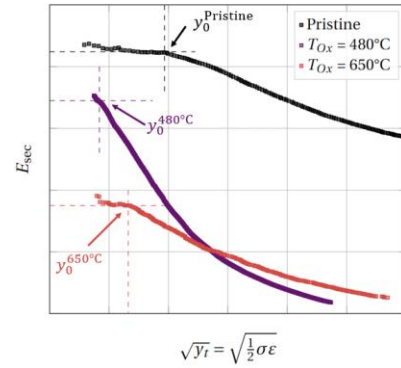


Figure 13. Evolution of the secant modulus during loading after oxidation as a function of the total energy.

Figure 12 shows the envelope of the behaviour curves. Linear elastic behaviour is at the beginning of the curves, followed by damaged behaviour. The damage threshold y_{0_i} can be measured graphically using Figure 13 from the point where the secant modulus drops.

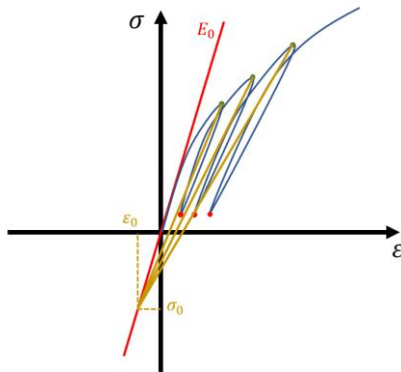


Figure 14. Definition of the closure strain.

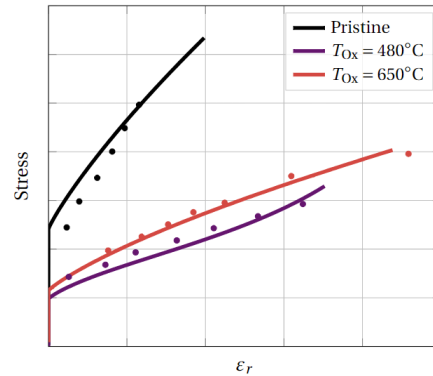


Figure 15. Identification of the closure strain using the measured permanent strains.

The damage threshold decreases as a function of oxidation, and appears to be lower at higher oxidation temperatures. This result needs to be confirmed by further measurements. An analysis of the effects of oxidation on the coefficients associated with the damage kinetics led to the conclusion that the damage saturation may not depend on the level of oxidation. The closure strain ε_0 , defined in Figure 14, allows a precise description of the permanent strain after unloading. To identify the value of ε_0 , the difference between the measured permanent strains, points reported in Figure 15, and those obtained numerically, lines in Figure 15, is minimized. Higher weights are affected to the measured large permanent strains in the minimization as their measurements are more reliable. Oxidation has therefore an important effect on the permanent strains. In addition, the closure strain allows residual strains to be accurately described in a simple manner.

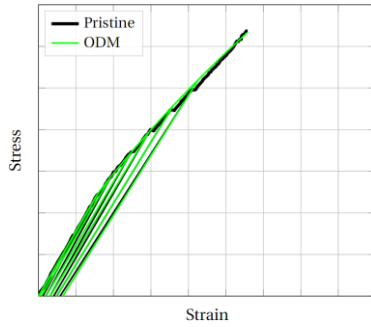


Figure 16. Stress-strain curve of the pristine material and the identified model.

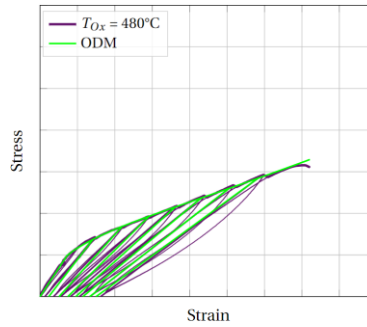


Figure 17. Stress-strain curve of the oxidized material ($T_{Ox} = 480^\circ C$, $\Delta m = 5\%$) and the identified model.

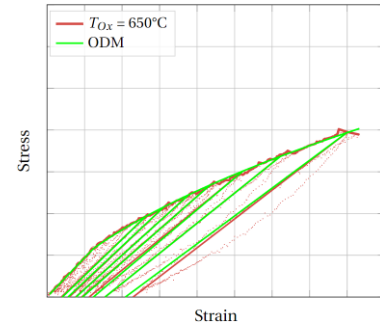


Figure 18. Stress-strain curve of the oxidized material ($T_{Ox} = 650^\circ C$, $\Delta m = 5\%$) and the identified model.

Once the damage threshold and closure strain have been identified graphically, the damage kinetics coefficient y_{c_i} can be determined. At this stage, all the coefficients are identified. The comparison between test and simulation for different oxidations can be seen in Figures 16 (pristine state with $\Delta m = 0\%$), 17 (oxidized at $480^\circ C$ with $\Delta m = 5\%$), and 18 (oxidized at $650^\circ C$ with $\Delta m = 5\%$) and the predictions are quite promising.

3. Conclusions

A formalism has been proposed to describe the oxidation state of C/C materials. For C/C materials, it has been established that for the same global mass loss, which is the commonly measured quantity to describe the oxidation state, is not fully relevant. Indeed, a high oxidation temperature degrades the elasticity tensor more than a low oxidation temperature for the same global mass loss. The main modeling idea is to assume that two oxidation mechanisms are in competition: at low temperatures, the mechanism noted $\Delta \dot{m}_1$ is larger than the mechanism $\Delta \dot{m}_2$, and vice versa at high temperatures. A Arrhenius-based model was proposed to predict the oxidation rate of each basic mechanism as a function of the oxidation time and the duration. Then, the effects of the oxidation states on the elastic properties but also on the damage indicators (onset of damage, permanent strain,) have been introduced in a continuum damage model. The predictions are in good agreement with the available experimental data, but additional tests are needed for validation.

In perspective, the effect of oxidation on the material parameters related to the damageable part of the model will be further investigated. This model is being implemented in a commercial finite element code. The effect of oxidation on fatigue behaviour will then be investigated.

References

- [1] J.-C. Cavalier et F. Christin, *Matériaux composites thermostructuraux*, Plast. Compos., 1992, doi: 10.51257/a-v1-a7804
- [2] Safran Landing Systems (safran-group.com)
- [3] A. Raude, *Modélisation thermomécanique d'un composite carbone/carbone à texture complexe*, PhD thesis, Université de Bordeaux, 2018
- [4] Mauchin, A. *Comportement mécanique à haute température de composites carbone/carbone*. PhD thesis, ENSIETA, 1997.
- [5] M. Fradin, G. Couégnat, F. Rebillat, K. Haras, et G. L. Vignoles, *Designing porous C/C composites for oxidation resistance with an analytical model based on the kinetic and architectural features of fibers and matrix*, Compos. Part B Eng., vol. 263, p. 110825, 2023
- [6] Cheng, T. *Understanding the ultra-high-temperature mechanical behaviors of advanced two-dimensional carbon-carbon composites*. Ceramics International, 46(13) :21395–21401., 2020
- [7] X. Bertran, C. Labrugère, M. A. Dourges, et F. Rebillat, *Oxidation Behavior of PAN-based Carbon Fibers and the Effect on Mechanical Properties*, Oxid. Met., vol. 80, no 3-4, p. 299-309, 2013
- [8] Maire, J. F. and Chaboche, J.-L. *A new formulation of Continuum Damage Mechanics (CDM) for composite materials*. Aerospace Science and Technology, (n°4) :247–257, 1997
- [9] Marcin, L. *Modélisation du comportement, de l'endommagement et de la rupture de matériaux composites à renforts tissés pour le dimensionnement robuste de structures*, PhD thesis, Université Bordeaux 1, 2010.
- [10] O. Sally, F. Laurin, C. Julien, R. Desmorat, et F. Bouillon, *Estimation de la rigidité résiduelle d'une structure composite oxyde/oxyde sollicitée en fatigue: comparaison essais/calculs*, 21^{ème} Journées Nationales sur les Composites, École Nationale Supérieure d'Arts et Métiers (ENSAM) - Bordeaux, Jul 2019, Bordeaux, Talence, France. hal-02420768.